



Backward bifurcation in a model for HTLV-I infection of CD4⁺ T cells

Horacio Gómez-Acevedo, Michael Y. Li*

Department of Mathematical and Statistical Sciences, University of Alberta, Edmonton, Alberta, T6G 2G1, Canada

Received 29 July 2003; accepted 18 June 2004

Abstract

Human T-cell Lymphotropic Virus Type I (HTLV-I) primarily infects CD4⁺ helper T cells. HTLV-I infection is clinically linked to the development of Adult T-cell Leukemia/Lymphoma and of HTLV-I Associated Myelopathy/Tropical Spastic Paraparesis, among other illnesses. HTLV-I transmission can be either horizontal through cell-to-cell contact, or vertical through mitotic division of infected CD4⁺ T cells. It has been observed that HTLV-I infection has a high proviral load but a low rate of proviral genetic variation. This suggests that vertical transmission through mitotic division of infected cells may play an important role. We consider and analyze a mathematical model for HTLV-I infection of CD4⁺ T cells that incorporates both horizontal and vertical transmission. Among interesting dynamical behaviors of the model is a backward bifurcation which raises many new challenges to effective infection control.

© 2004 Society for Mathematical Biology. Published by Elsevier Ltd. All rights reserved.

1. Introduction

Human T-cell Lymphotropic Virus Type I (HTLV-I) infection is responsible for several diseases such as Adult T-cell Leukemia/Lymphoma (ATL) and HTLV-I Associated Myelopathy/Tropical Spastic Paraparesis (HAM/TSP) (Cann and Chen, 1996). As a retrovirus, HTLV-I uses reverse transcriptase to synthesize DNA segments (provirus)

* Corresponding author.
E-mail address: mli@math.ualberta.ca (M.Y. Li).

that integrate into the host DNA. The main target for the viral infection is the CD4⁺ T-lymphocyte population (Cann and Chen, 1996; Grant et al., 2002). Unlike the HIV, which can break free from host cells and infect other T cells, cell-free HTLV-I does not trigger infection (Wucherpfennig et al., 1992). Cell-to-cell contact is normally required to transmit the infection among CD4⁺ T cells (Cann and Chen, 1996; Grant et al., 2002). Like other retroviruses, HTLV-I provirus can also be vertically transmitted to the daughter cells of an infected cell during mitosis (Bangham, 2000; Mortreux et al., 2003).

The proportion of provirus-containing cells in HTLV-I infection is remarkably high; typically between 0.1% and 10% of peripheral blood mononuclear cells harbor HTLV-I provirus, and this percentage can be as high as 20% in HAP/TSP patients (Cann and Chen, 1996; Bangham, 2000; Grant et al., 2002). It requires a considerable level of viral replication to obtain such proviral load. During the mitotic division, proviruses in an HTLV-I infected T cell are replicated by the host DNA polymerase, and the rate of mutation is considerably low. In contrast, the action of viral reverse transcriptase is error-prone and accumulates sequence variations rapidly. HTLV-I exhibits an extraordinary genetic stability (Cann and Chen, 1996; Bangham et al., 1999). This apparent discrepancy between a high proviral load and low genetic variability suggests that mitotic transmission may play a relevant and even important role in the persistence of the HTLV-I infection (Bangham et al., 1999; Mortreux et al., 2001, 2003).

To model the HTLV-I infection of CD4⁺ T cells, we partition the T-cell population into uninfected and infected classes. Let $x(t)$, $y(t)$ denote the number of uninfected and infected cells at time t , respectively. We assume that the proliferation of T cells due to mitotic division obeys a logistic growth. The mitotic proliferation of uninfected cells is described by $v_1 x(t)[1 - (x(t) + y(t))/K]$, where v_1 is the proliferation constant and K is the level at which mitotic division of CD4⁺ T cells stops. Infected cells retain most of the cellular functionalities (Cann and Chen, 1996), their division is assumed to be similar to that of the uninfected cells, and is described by $v_2 y(t)[1 - (x(t) + y(t))/K]$, with proliferation constant v_2 . The horizontal transmission of HTLV-I is through cell-to-cell contact between infected and uninfected cells, and, following Wodarz et al. (1999) and Nowak and May (2000), is assumed to have a bilinear incidence form $\beta x(t)y(t)$, where β is the transmission coefficient. Newly infected CD4⁺ T cells face a strong humoral immune response (Bangham, 2000). We assume that only a fraction σ of cells newly infected by direct contact escape the immune system attack, and are able to infect other T cells. Here $0 \leq \sigma \leq 1$. We assume that the body generates CD4⁺ T cells at a constant rate λ and newly generated cells are uninfected. The removal rate of uninfected CD4⁺ T cells is a constant μ_1 , and may include the loss due to natural death and activation by a nonHTLV-I antigen. The removal rate for infected cells, μ_2 , may include the loss due to natural causes and cell-mediated immune response.

The model is described by the following system of nonlinear differential equations

$$\begin{aligned} x' &= \lambda + v_1 x \left(1 - \frac{x + y}{K}\right) - \mu_1 x - \beta xy, \\ y' &= \sigma \beta xy + v_2 y \left(1 - \frac{x + y}{K}\right) - \mu_2 y. \end{aligned} \tag{1}$$

Adding the two equations and using $N = x + y$ we obtain

$$(x + y)' \leq \lambda + \nu(x + y) \left(1 - \frac{x + y}{K}\right) - \mu(x + y),$$

where $\nu = \max\{\nu_1, \nu_2\}$ and $\mu = \min\{\mu_1, \mu_2\}$. It follows that $\limsup_{t \rightarrow \infty} x(t) + y(t) \leq \bar{N}$ where $N = \bar{N}$ is the positive root of the quadratic equation $\lambda + (\nu - \mu)N - \frac{\nu}{K}N^2 = 0$. Thus a feasible region for (1) is

$$\Gamma = \{(x, y) \in \mathbb{R}_+^2 : x + y \leq \bar{N}\}.$$

It can be shown that Γ is positively invariant with respect to (1).

We present a detailed mathematical analysis of the bifurcation and global dynamics of (1) in Γ . The analysis mainly involves phase-plane analysis, and can be easily followed by mathematicians and theoretical biologists. Under assumptions that are biologically sound, we show that a backward bifurcation occurs: multiple stable equilibria exist for an open set of parameter values, when the basic reproduction number is below one. Implications of our mathematical results to the immunological process of HTLV-I infection, and the biological significance of backward bifurcation will be discussed in the Discussion section at the end of the paper.

2. Equilibria and backward bifurcation

An equilibrium (x, y) satisfies

$$\begin{aligned} 0 &= \lambda + \nu_1 x \left(1 - \frac{x + y}{K}\right) - \mu_1 x - \beta xy, \\ 0 &= \sigma \beta xy + \nu_2 y \left(1 - \frac{x + y}{K}\right) - \mu_2 y. \end{aligned} \tag{2}$$

The *infection-free equilibrium* $P_0 = (x_0, 0)$ exists for all parameter values, where $x_0 > 0$ is the positive root of the polynomial

$$f_1(x) = \lambda + (\nu_1 - \mu_1)x - \frac{\nu_1}{K}x^2. \tag{3}$$

A *chronic-infection equilibrium* $\bar{P} = (\bar{x}, \bar{y})$ satisfies (2) with $\bar{y} > 0$. From the second equation of (2) we obtain

$$\bar{y} = \frac{K}{\nu_2} \left[\left(\sigma \beta - \frac{\nu_2}{K} \right) \bar{x} + (\nu_2 - \mu_2) \right]. \tag{4}$$

Substituting this into the first equation of (2), we conclude that an chronic-infection equilibrium satisfies

$$f_1(\bar{x}) = f_2(\bar{x}),$$

where f_1 is defined in (3) and

$$f_2(x) = \frac{1}{\nu_2} \left(\frac{\nu_1}{K} + \beta \right) [(\sigma K \beta - \nu_2)x + K(\nu_2 - \mu_2)]x. \tag{5}$$

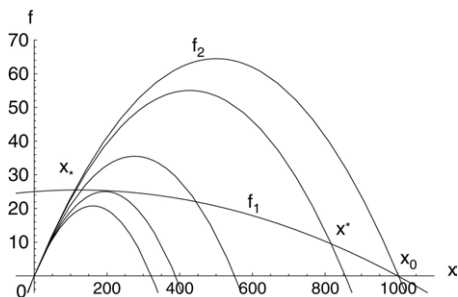


Fig. 1. As σ varies from 0 to 1, the graph of f_2 varies and the number of intersections of f_1 and f_2 changes from 0 to 1, then to 2 and back to 1. The parameter values are chosen as in Section 4. The five graphs of f_2 shown correspond to $\sigma = 0.007, 0.0125, 0.018, 0.023,$ and 0.0243 , with the rest of the parameter values fixed.

The number of chronic-infection equilibria can be analyzed geometrically through intersections of the graphs of f_1 and f_2 . System (1) can have more than one chronic-infection equilibria only if f_2 is concave down and has a positive root. This happens if and only if the following condition holds:

$$\sigma K\beta < \nu_2 \quad \text{and} \quad \mu_2 < \nu_2. \tag{6}$$

Since our primary interest is to explore occurrence of backward bifurcation in system (1), we will assume condition (6) holds throughout the paper. It has been reported (Bangham, 2000) that a strong humoral immune response to HTLV-I is established within months after the infection. Moreover, the HTLV-I proviral load consists of relatively few clones (Mortreux et al., 2003). It is reasonable to expect that the fraction of cells that are infected by direct contact and survive the immune system attack is small, namely $\sigma \ll 1$. On the other hand, the high proviral load of HTLV-I infection suggests that replication via mitosis contributes significantly. It is therefore not unreasonable to expect that the growth constant ν_2 for mitosis of infected T cells dominates the natural death rate μ_2 . The parameter range defined by (6) is biologically sound.

To ensure that the graphs of f_1 and f_2 intersect for some range of σ , we require the following technical condition

$$(\nu_1 + \beta K)^2 \left(1 - \frac{\mu_2}{\nu_2}\right)^2 > (\nu_1 - \mu_1)^2 + 4\lambda \frac{\nu_1}{K}, \tag{7}$$

which is derived from the condition $f_2'(x_0) > f_1'(x_0)$, see Fig. 1. We will show, in Section 4, that (7) can be satisfied by parameter values that are realistic for human HTLV-I infection.

Define

$$\sigma_0 = \frac{4\lambda\beta\nu_2^2 - [(\nu_1 - \mu_1)\nu_2 - (\nu_1 + K\beta)(\nu_2 - \mu_2)]^2}{4\lambda\beta\nu_2(\nu_1 + K\beta)} \tag{8}$$

and

$$\sigma_c = \frac{\nu_2}{K\beta} - \frac{(\nu_2 - \mu_2)}{\beta x_0}. \tag{9}$$

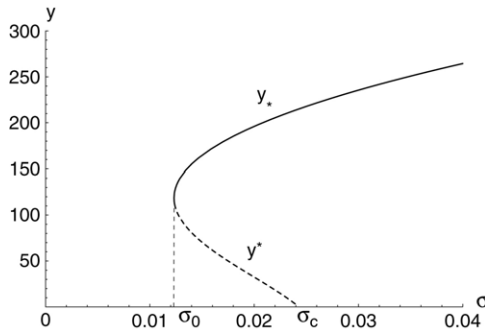


Fig. 2. Bifurcation diagram of (1) showing a backward bifurcation, as σ varies from 0 to 0.04. The other parameter values are chosen as in Section 4. Note $R_0(\sigma_c) = 1$.

We assume that

$$0 \leq \sigma_0 < \sigma_c < 1. \tag{10}$$

As parameter σ varies, the number of chronic equilibria is shown in the following four cases (see Fig. 1):

- (i) If $0 < \sigma < \sigma_0$, graphs of f_1 and f_2 do not intersect, and there is no chronic-infection equilibrium.
- (ii) If $\sigma = \sigma_0$, the graphs of f_1 and f_2 are tangent, and there is a unique chronic-infection equilibrium.
- (iii) If $\sigma_0 < \sigma < \sigma_c$, there are two chronic-infection equilibria, $P_* = (x_*, y_*)$ and $P^* = (x^*, y^*)$, $x_* < x^*$, $y_* > y^*$. These are the two intersections of graphs of f_1 and f_2 in the first quadrant.
- (iv) If $\sigma \geq \sigma_c$ there is a unique chronic-infection equilibrium $P_* = (x_*, y_*)$ in the feasible region Γ . In this case, graphs of f_1 and f_2 have only one intersection in the first quadrant. The value σ_c is such that $x^* = x_0$. Also the condition (7) implies that $|f_1'(x_0)| < |f_2'(x_0)|$ when $\sigma = \sigma_c$, so that the graph of f_2 is above that of f_1 to the left of and close to x_0 .

We summarize the preceding analysis in the following result. The corresponding bifurcation diagram is shown in Fig. 2.

Theorem 2.1. *System (1) always has the infection-free equilibrium $P_0 = (x_0, 0)$. Assume that conditions (6), (7) and (10) are satisfied. Then the number of chronic-infection equilibria is determined by σ . More specifically,*

- (i) *If $0 < \sigma < \sigma_0$, there is no chronic-infection equilibria.*
- (ii) *If $\sigma = \sigma_0$, there is a unique chronic-infection equilibrium.*
- (iii) *If $\sigma_0 < \sigma < \sigma_c$, there are two chronic-infection equilibria P_* and P^* .*
- (iv) *If $\sigma \geq \sigma_c$, there is a unique chronic-infection equilibrium P_* .*

The basic reproductive number for the infection of HTLV-I is the average number of secondary infections caused by a single infected CD4⁺ T cell introduced in an entirely susceptible CD4⁺ T-cell population, over its entire infectious period $1/\mu_2$. For our model (1), the basic reproduction number $R_0 = R_0(\sigma)$ is given as follows

$$R_0(\sigma) = \frac{1}{\mu_2} \left[\sigma\beta x_0 + \nu_2 \left(1 - \frac{x_0}{K} \right) \right]. \tag{11}$$

The first term in the brackets describes the per-unit-time secondary infections through the cell-to-cell contact, and the second term those through mitotic division. From its definition, we see that $R_0(\sigma)$ is an increasing function of σ . Furthermore, $R_0(\sigma_c) = 1$ by (9) and (11).

The bifurcation diagram in Fig. 2 shows the standard features of a ‘backward bifurcation’ [cf. Dushoff (1996), Dushoff et al. (1998), Greenhalgh et al. (2000), Haderl and van den Driessche (1997), Kribs-Zaleta and Martcheva (2002), Kribs-Zaleta and Velasco-Hernandez (2000), Martcheva and Thieme (2003), Medley et al. (2001), van den Driessche and Watmough (2000)]; multiple chronic-infection equilibria exists when the basic reproduction number is below unity. Such a bifurcation possesses certain ‘catastrophic’ behaviors:

- When $R_0(\sigma)$ increases through $1(R_0(\sigma_c))$, the number of infected cells can suddenly change from low level to a high persistent level. This may result in a sudden explosion of the infected cell population.
- When R_0 decreases through 1, the level of chronic-infection remains high.

This is in sharp contrast to the standard forward bifurcation in virus-host and epidemic models. A serious complication associated with a backward bifurcation is the following: lowering the basic production number R_0 below unity may no longer be a viable control measure, hence different prevention and control measures may have to be considered. We will come back to this subject in the Discussion section of the paper.

3. Stability of equilibria and global dynamics

Proposition 3.1. *The infection-free equilibrium $P_0 = (x_0, 0)$ is locally asymptotically stable if $R_0(\sigma) < 1$, and is a saddle if $R_0(\sigma) > 1$.*

Proof. The Jacobian matrix of (1) at $P_0 = (x_0, 0)$ is

$$J(P_0) = \begin{pmatrix} \nu_1 \left(1 - \frac{x_0}{K} \right) - \frac{\nu_1 x_0}{K} - \mu_1 & -\frac{\nu_1 x_0}{K} - \beta x_0 \\ 0 & \mu_2 (R_0(\sigma) - 1) \end{pmatrix}.$$

Its two eigenvalues are $\nu_1 \left(1 - \frac{x_0}{K} \right) - \frac{\nu_1 x_0}{K} - \mu_1 = f'_1(x_0) < 0$, by (3) and the graph of f_1 , and $\mu_2 (R_0(\sigma) - 1)$, which has the same sign as $R_0(\sigma) - 1$. This establishes the proposition. □

The next result describes the stability of chronic-infection equilibria. Its proof is given in the [Appendix](#).

Proposition 3.2. (i) *If $\sigma_0 < \sigma < \sigma_c$, then P_* is locally asymptotically stable whereas P^* is a saddle.* (ii) *If $\sigma > \sigma_c$, then P_* is locally asymptotically stable.*

The stability properties of equilibria are indicated in the bifurcation diagram in Fig. 2, where solid lines indicate stable equilibria, and dotted lines indicate unstable equilibria. Note that in Fig. 2, P^* has a smaller y^* and lies in the middle branch, and P_* , with a larger y_* , lies on the top branch. Also note that $R_0 = R_0(\sigma)$ increases with σ and $R_0(\sigma_c) = 1$. Thus $\sigma_0 < \sigma < \sigma_c \iff R_0(\sigma_0) < R_0(\sigma) < 1$, and $\sigma > \sigma_c \iff R_0(\sigma) > 1$. We see that $R_0(\sigma)$ still behaves as a threshold parameter in that if $R_0(\sigma) < 1$, the infection-free equilibrium P_0 is stable, whereas if $R_0(\sigma) > 1$, P_0 becomes unstable and a unique chronic-infection equilibrium P_* is stable. However, the peculiarity of the backward bifurcation, as shown in Fig. 2, is that a stable chronic-infection equilibrium coexists with the stable infection-free equilibrium P_0 , when $R_0(\sigma)$ is below 1. The coexisting attractors and their basins of attraction are further described in the next result, which establishes the global dynamics of (1). The proof is given in the Appendix.

Theorem 3.3. *Assume that conditions (6), (7) and (10) are satisfied. Then*

- (i) *when $0 < R_0 < R_0(\sigma_0)$, the infection-free equilibrium P_0 is globally asymptotically stable in $\bar{\Gamma}$;*
- (ii) *when $R_0(\sigma_0) < R_0 < 1$, system (1) has two attractors in $\bar{\Gamma}$, the infection-free equilibrium P_0 and the chronic-infection P_* . Their basins of attraction in $\bar{\Gamma}$ are separated by the stable manifolds of the saddle point P^* ;*
- (iii) *when $R_0 > 1$, the unique chronic-infection equilibrium P_* is globally asymptotically stable in $\bar{\Gamma}$.*

In Fig. 3, a phase-portrait of (1) for case (ii) of Theorem 3.3 is numerically generated using *Mathematica*, using parameter values as chosen in Section 4. Three equilibria are marked as dots, with P_0 on the x -axis and P^* sitting between P_* and P_0 . The heteroclinic orbits from P^* to P_* and P_0 are clearly identifiable, so are the basin boundaries, which are the stable manifolds of the saddle point P^* . In this case, $R_0(\sigma) < 1$, but the fate of an infection critically depends on the initial conditions. If the initial point lies in the basin of attraction of P_0 , then the infection will die out, whereas the infection will persist if the initial point lies in the basin of attraction of P_* . This behavior does not occur in virus-host models that have only the forward bifurcation [cf. Gómez-Acevedo and Li (2002), Wang et al. (2002)].

4. Parameter values and numerical simulations

Conditions (6), (7) and (10) define an open region in the parameter space for backward bifurcation and bistability to occur in system (1). In this section, we give some biologically relevant conditions that ensure (6), (7) and (10). We first assume that healthy and infected T cells have similar natural growth and death rates:

$$\mu_1 \doteq \mu_2, \quad \nu_1 \doteq \nu_2. \tag{12}$$

Here and in the rest of this section, ‘ \doteq ’ denotes ‘approximately equals’. We expect that, when infection is absent, the equilibrium level x_0 of T cells is less than the carrying

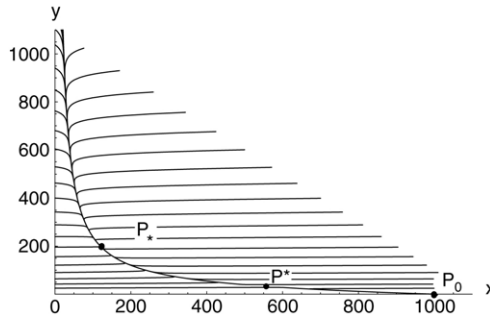


Fig. 3. A phase portrait of (1) showing a stable chronic-infection equilibrium P_* and the stable infection-free equilibrium P_0 .

capacity K , namely

$$x_0 < K. \tag{13}$$

We choose the time unit in system (1) as day and follow a scaling law suggested by Perelson (1989):

$$\beta K \doteq 1 \text{ (day)}. \tag{14}$$

We assume

$$\sigma < \nu_2, \quad \mu_i < \nu_i < 1, \quad i = 1, 2. \tag{15}$$

Here $\sigma < \nu_2, \mu_i < \nu_i, i = 1, 2$ agree with (6), under (12) and (14), while $\nu_i < 1, i = 1, 2$ are expected given our choice of time unit, and are satisfied by CD4⁺ T cell data in the literature, see discussion later in this section. Finally we assume that $\nu_1 - \mu_1$ and $\nu_2 - \mu_2$ are in the following range

$$\mu_1 \nu_1 < \frac{\nu_1 - \mu_1}{2} < \sqrt{\frac{\lambda}{K}} \nu_1. \tag{16}$$

It can be shown that conditions (12)–(16) imply (6), (7) and (10). A proof is given in the Appendix. We thus have established the following result.

Corollary 4.1. *Conclusions of Theorems 2.1 and 3.3 hold under the assumptions (12)–(16).*

Conditions (12)–(16) are biologically relevant and easy to use when parameters are selected for simulations. We also want to comment that part of the inequality (16)

$$\frac{\nu_1 - \mu_1}{2} < \sqrt{\frac{\lambda}{K}} \nu_1$$

is required to ensure $\sigma_0 > 0$. In fact this requirement is not essential for our results, since, if $\sigma_0 \leq 0$ then the stable P_* branch in the bifurcation diagram will exist for all $R_0(\sigma) > 0$, and the infection always has a chance to persist. As long as $\sigma_c > 0$, there still exists a region of bistability.

Data in the literature can be used to show that parameter region for backward bifurcation that is defined by (6) and (7) is realistic for human HTLV-I infection. Based on parameter values in Nelson et al. (2000) for studies of HIV infection of CD4⁺ T cells, we choose the rate of production of CD4⁺ T cells as $\lambda = 25 \text{ cells mm}^{-3}$, and the natural death rate of CD4⁺ T cells as $\mu_2 = \mu_1 \doteq 0.03 \text{ day}^{-1}$. In the absence of HTLV-I infection, the number of CD4⁺ T cells is expected to be constant and has a normal count around $1000 \text{ cells mm}^{-3}$ (Nelson et al., 2000), and a carrying capacity constant $K = 1150 \text{ mm}^{-3}$. This gives us $x_0 \doteq 1000 \text{ mm}^3$, or $f_1(1000) \doteq 0$. Using (3) we can then estimate that the proliferation constant for the CD4⁺ T cells as $\nu_2 = \nu_1 \doteq 0.038 \text{ day}^{-1}$. To estimate β , we use the scaling relation (14), $\beta K \doteq 1 \text{ day}$. We choose $\beta = 1.03 \times 10^{-3} \text{ mm}^3/\text{cells}/\text{day}$. One can verify that, with these parameter values, condition (7) holds, and condition (6) gives a range (0, 0.038) of σ for backward bifurcation to occur. Furthermore, $\sigma_c = 0.024$, $\sigma_0 = 0.00007$, and $R_0(\sigma_0) = 0.169$. Therefore, infection is able to persist at an equilibrium level if $R_0 > 0.169$. Equivalently, total infection control is achieved only if $R_0 < 0.169$.

Numerical simulations of the model using these parameter values are carried out on *Mathematica*. In Fig. 4(a) and (b), $\sigma = 0.015$ and $R_0 = 0.68$ are in the range of bistability, and we see that small initial infection leads to total recovery in Fig. 4(a), and higher initial infection leads to persistent infection in Fig. 4(b). In Fig. 4(c), all parameter values are the same as in Fig. 4(a) and (b) except $\sigma = 0.03$ and $R_0 = 1.17$, which belong to the persistence range. We see that even a low initial infection leads to persistent infection in this case. These simulations also show that persistent infection will produce a proviral load in the range of 10–20%, which is consistent with clinical data (Cann and Chen, 1996; Bangham, 2000; Grant et al., 2002).

In Fig. 5, simulations are run to demonstrate the catastrophic effect of the backward bifurcation. The same set of parameter values are used. We choose $\sigma = 0.0238$, slightly less than $\sigma_c = 0.024$. In Fig. 5(a), $R_0 = 0.96$, $y(0) = 10$, and infection level remains low for 2000 days. In Fig. 5(b), $\sigma = 0.0238$ remains the same, and we lower μ_2 from 0.03 to 0.015 so that $R_0 = 1.43$. The same initial infection level $y(0) = 10$ leads to a huge jump in infection level within a year.

5. Discussion

It is known that HTLV-I infection of CD4⁺ T cells is through direct cell-to-cell contact (Wucherpfennig et al., 1992; Cann and Chen, 1996; Grant et al., 2002). Current clinical research supports the following theory [see Bangham (2000), Mortreux et al. (2001, 2003), Wattel et al. (1995)]: the HTLV-I infection consists of two steps; a transient phase of reverse transcription and a phase of persistent multiplication of infected CD4⁺ T cells. When an infected T cell multiplies, proviruses can be passed to the genome of the daughter cells, as a form of vertical transmission. This two-step process can explain the observed high proviral load and low genetic variability in HTLV-I infected T cells. In this paper, we propose and analyze a mathematical model for the infection of CD4⁺ T cells by HTLV-I based on this two-step process theory. The model incorporates both horizontal transmission through cell-to-cell contact and vertical transmission through mitotic division of infected T cells. We also assume a fraction σ of the infected cells survive the immune system attack after the

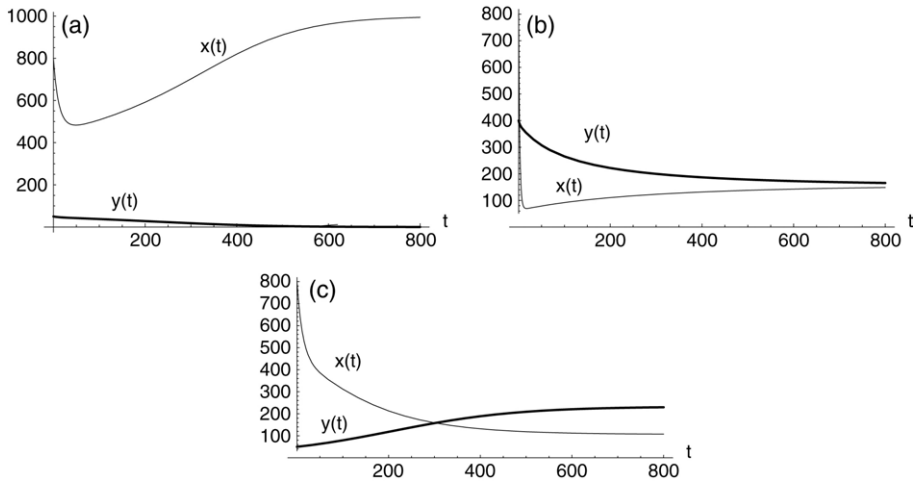


Fig. 4. Mathematica simulations of system (1) with parameter values $\mu_1 = \mu_2 = 0.03$, $\nu_1 = \nu_2 = 0.038$, $\lambda = 25$, $K = 1150$, $\beta = 0.00103$, $x_0 = 1000$. (a) and (b) show, when $\sigma = 0.015$ and $R_0 = 0.68$, the fate of the infection depends on the initial condition due to the bistability. (c) shows, when $\sigma = 0.03$ and $R_0 = 1.17$, infection persists even when $y(0) = 50$. The persistent infection shows a proviral load level of 16%.

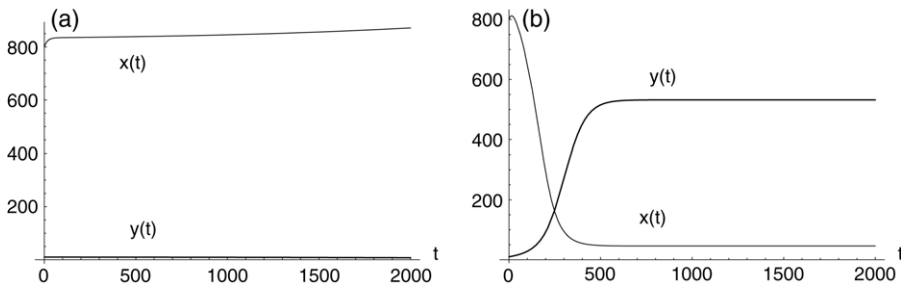


Fig. 5. Mathematica simulations that show a sudden jump of infection level with small change in R_0 . Parameter values used are $\mu_1 = 0.03$, $\nu_1 = \nu_2 = 0.038$, $\lambda = 25$, $K = 1150$, $\beta = 0.00103$, $x_0 = 1000$, $\sigma = 0.0238$. In (a), $\mu_2 = 0.03$, $R_0 = 0.96$, infection remains low. In (b), $\mu_2 = 0.02$, $R_0 = 1.43$, infection level has a sudden jump.

error prone viral replication. The genetic stability of HTLV-I suggests that the fraction σ should be very low ($\sigma \ll 1$). Also, the high proviral load in HTLV-I infection suggests that rate of the mitotic division should be high ($\nu_2 > \mu_2$). Under these biologically sound assumptions, our model has a bifurcation diagram that predicts persistent infection for an extended range of the basic reproduction number $R_0 > R_0(\sigma)$. This verifies the two-step process theory. However, somewhat surprisingly, the same bifurcation diagram shows that the model undergoes a backward bifurcation as σ increases: a stable chronic-infection equilibrium P_* exists when the basic reproduction number $R_0(\sigma)$ is below unity for an open range of parameter values. The global dynamics for the corresponding parameter range show that P_* and the infection-free equilibrium P_0 are co-existing attractors whose basins of attraction partition the feasible region. Even when the basic reproduction number

$R_0(\sigma) < 1$, whether an infection persists or dies out critically depends on if the initial point lies in the basin of attraction of P_* or that of P_0 , respectively. This clearly demonstrates the catastrophic behavior that accompanies the backward bifurcation.

Backward bifurcation in compartmental models has only recently attracted serious research attention. Several mechanisms have been shown to lead to backward bifurcation in epidemic models, see Dushoff (1996), Dushoff et al. (1998), Greenhalgh et al. (2000), Haderler and van den Driessche (1997), Kribs-Zaleta and Martcheva (2002), Kribs-Zaleta and Velasco-Hernandez (2000), Martcheva and Thieme (2003), Medley et al. (2001) and van den Driessche and Watmough (2000). Dushoff et al. (1998) provided an intuitive general mechanism for backward bifurcation to occur: an increase in infected population does not lead to a decrease in susceptibles. In our model, vertical transmission through mitotic division allows the infected to grow without decreasing uninfected. This seems to agree with the intuition in Dushoff et al. (1998). We want to comment, however, that the loss of infected T cells due to immune response after viral replication is also important; backward bifurcation does not occur in our model when $\sigma = 1$. When $\sigma = 1$, our model is the same as a SI epidemic model with immigration and logistic growth, and bilinear incidence. It is known that such a model only has forward bifurcation and no bi-stability occurs, see Pugliese (1990). In this sense, our analysis indicates that backward bifurcation is a byproduct of the two-step process of the HTLV-I infection.

In a standard forward bifurcation [cf. Gómez-Acevedo and Li (2002), Wang et al. (2002)], when R_0 passes through 1, the level of chronic infection remains low. In contrast, as demonstrated in the bifurcation diagram in Fig. 2, a backward bifurcation results in the following catastrophic effects:

- When R_0 increases through 1, the number of infected T-cell population may experience a sudden explosion.
- When R_0 decreases through 1, the level of chronic-infection remains high.

As a result, the standard infection-control measure of lowering R_0 to below 1 is no longer viable; R_0 needs to be below $R_0(\sigma_0)$ to achieve infection control, which may be very difficult. Other infection-control measures need to be investigated. Based on our model and analysis, such measures may include:

- lower the level of chronic infection y_* to unharmed levels;
- increase the value $R_0(\sigma_0)$ to close to 1, and hence reduce the parameter range for backward bifurcation to occur;
- identify basin of attractions and basin boundaries as shown in Fig. 3. This may help to design tests for development of chronic infection.

In conclusion, our model and analysis suggests that backward bifurcation may be intrinsic to the HTLV-I infection dynamics. An interesting recent study on the hepatitis-B virus infection by Medley et al. (2001) shows the occurrence of a backward bifurcation and calls for a re-evaluation of public health policy towards hepatitis-B. Our theoretical results warrant further investigation of the HTLV-I infection dynamics using more realistic models and through verification by clinical data.

Acknowledgements

The authors would like to thank Professor J.M. Murray of University of New South Wales for his help with this research. Comments by an anonymous referee helped to improve the paper and are greatly appreciated. Gómez-Acevedo acknowledges support from the NCE-MITACS Project ‘Mathematical Modeling in Pharmaceutical Development’. Li’s research is supported in part by grants from the Natural Science and Engineering Research Council of Canada, Canada Foundation for Innovation, and the National Science Foundation of the US.

Appendix

Proof of Proposition 3.2. The Jacobian matrix $J(\bar{P})$ of (1) at a chronic-infection equilibrium point $\bar{P} = (\bar{x}, \bar{y})$ is

$$\begin{pmatrix} v_1 \left(1 - \frac{\bar{x} + \bar{y}}{K}\right) - \frac{v_1 \bar{x}}{K} - \mu_1 - \beta \bar{y} & -\frac{v_1 \bar{x}}{K} - \beta \bar{x} \\ \left(\sigma \beta - \frac{v_2}{K}\right) \bar{y} & \sigma \beta \bar{x} + v_2 \left(1 - \frac{\bar{x} + \bar{y}}{K}\right) - \frac{v_2 \bar{y}}{K} - \mu_2 \end{pmatrix}.$$

By the equilibrium equation (2),

$$\begin{aligned} \text{tr } J(\bar{P}) &= v_1 \left(1 - \frac{\bar{x} + \bar{y}}{K}\right) - \frac{v_1 \bar{x}}{K} - \mu_1 - \beta \bar{y} \\ &\quad + \sigma \beta \bar{x} + v_2 \left(1 - \frac{\bar{x} + \bar{y}}{K}\right) - \frac{v_2 \bar{y}}{K} - \mu_2 = -\frac{\lambda}{\bar{x}} - \frac{v_1 \bar{x}}{K} - \frac{v_2 \bar{y}}{K} < 0. \end{aligned}$$

Thus $\text{tr } J(\bar{P}) < 0$ for both $\bar{P} = P_*$ and $\bar{P} = P^*$. Also, using the definition of f_1 and f_2 in (3) and (5), respectively, we obtain

$$\begin{aligned} \det J(\bar{P}) &= \left(f'_1(\bar{x}) - \left(\frac{v_1}{K} + \beta\right) \bar{y}\right) \left(-\frac{v_2 \bar{y}}{K}\right) + \left(\frac{v_1}{K} + \beta\right) \left(\sigma \beta - \frac{v_2}{K}\right) \bar{x} \bar{y} \\ &= \bar{y} \left[-\frac{v_2}{K} f'_1(\bar{x}) + \frac{v_2}{K} \left(\frac{v_1}{K} + \beta\right) \bar{y} + \left(\frac{v_1}{K} + \beta\right) \left(\sigma \beta - \frac{v_2}{K}\right) \bar{x}\right] \\ &= \bar{y} \left[-\frac{v_2}{K} f'_1(\bar{x}) + \left(\frac{v_1}{K} + \beta\right) (v_2 - \mu_2) + 2 \left(\frac{v_1}{K} + \beta\right) \left(\sigma \beta - \frac{v_2}{K}\right) \bar{x}\right] \\ &= \bar{y} \frac{v_2}{K} (-f'_1(\bar{x}) + f'_2(\bar{x})). \end{aligned}$$

Note that $f'_2(x) - f'_1(x) > 0$ when $x = x_*$ and $f'_2(x) - f'_1(x) < 0$ when $x = x^*$. We know that P_* is locally asymptotically stable whenever it exists, and P^* is a saddle whenever it exists. This establishes Proposition 3.2. \square

Proof of Theorem 3.3. We first rule out periodic orbits in $\overset{\circ}{\Gamma}$ using Dulac’s criteria [see Brauer and Noel (1968), Hale (1969)]. We choose a Dulac multiplier $\alpha(x, y) = 1/xy$. Let $(P(x, y), Q(x, y))$ denote the right-hand-side of (1). We have

$$\frac{\partial(\alpha P)}{\partial x} + \frac{\partial(\alpha Q)}{\partial y} = -\left(\frac{\lambda}{x^2 y} + \frac{v_1}{K y} + \frac{v_2}{K x}\right) < 0,$$

for all $x > 0, y > 0$. Thus (1) has no periodic orbits in \overline{T} . A simple application of the classical Poincaré–Bendixson theory shows that all solutions in \overline{T} converge to a single equilibrium. This establishes the claims in the theorem. \square

Proof of Corollary 4.1. From (3) and (9), and using (12) and the equation

$$\frac{v_1}{K}x_0^2 - (v_1 - \mu_1)x_0 - \lambda = 0, \tag{A.1}$$

we have

$$\beta\sigma_c = \frac{v_2}{K} - \frac{v_2 - \mu_2}{x_0} \doteq \frac{v_1}{K} - \frac{v_1 - \mu_1}{x_0} = \frac{\lambda}{x_0^2} > 0.$$

Thus

$$0 < \sigma_c < \frac{v_2}{\beta K} \doteq v_2 < 1,$$

by (14) and (15). From (8), (12) and (14) we obtain

$$\sigma_0 \doteq \frac{1}{4\lambda v_1(v_1 + \beta K)} [4\lambda v_1^2 - (v_1 - \mu_1)^2 K] > 0$$

by (16). Using (13) and (16) we can show

$$(v_1 + 1) \left(1 - \frac{\mu_1}{v_1} \right) > v_1 + \mu_1 > \frac{2v_1 x_0}{K} - (v_1 - \mu_1).$$

This relation, together with the quadratic formula for Eq. (A.1), leads to

$$(v_1 + 1) \left(1 - \frac{\mu_1}{v_1} \right) > \sqrt{(v_1 - \mu_1)^2 + \frac{4\lambda v_1}{K}},$$

and thus by conditions (12) and (14), we arrive at relation (7). Since condition (7) implies that the graphs of f_1 and f_2 have two intersections at $\sigma = \sigma_c$, while $\sigma_0 > 0$ implies that the graphs of f_1 and f_2 have no intersection at $\sigma = 0$, continuous dependence of these graphs on σ implies that $0 < \sigma_0 < \sigma_c$, hence the relation (10). \square

References

- Bangham, C.R.M., 2000. The immune response to HTLV-I. *Curr. Opin. Immunol.* 12, 397–402.
- Bangham, C.R.M., Hall, S.E., Jeffery, K.J.M., Vine, A.M., Witkover, A., Nowak, M.A., Usuku, K., Osame, M., 1999. Genetic control and dynamics of the cellular immune response to the human T-cell leukemia virus, HTLV-I. *Philos. Trans. R. Soc. Lond. B Biol. Sci.* 354, 691–700.
- Brauer, F., Noel, J.A., 1968. *Qualitative Theory of Ordinary Differential Equations*. Benjamin, New York.
- Cann, A.J., Chen, I.S.Y., 1996. Human T-cell leukemia virus types I and II. In: Fieds, B.N., Knipe, D.M., Howley, P.M. et al. (Eds.), *Fields Virology*, 3rd edn. Lippincott-Raven Publishers, Philadelphia, pp. 1849–1880.
- Dushoff, J., 1996. Incorporating immunological ideas in epidemiological models. *J. Theor. Biol.* 180, 181–187.
- Dushoff, J., Huang, W., Castillo-Chavez, C., 1998. Backwards bifurcations and catastrophe in simple models of fatal diseases. *J. Math. Biol.* 36, 227–248.
- Gómez-Acevedo, H., Li, M.Y., 2002. Global dynamics of a mathematical model for HTLV-I infection of T cells. *Canad. Appl. Math. Quart.* 10, 71–86.

- Grant, C., Barmak, K., Alefantis, T., Yao, J., Jacobson, S., Wigdahl, B., 2002. Human T cell leukemia virus type I and neurologic disease: events in bone marrow, peripheral blood, and central nervous system during normal immune surveillance and neuroinflammation. *J. Cell. Phys.* 190, 133–159.
- Greenhalgh, D., Diekmann, O., de Jong, M.C.M., 2000. Subcritical endemic steady states in mathematical models for animal infections with incomplete immunity. *Math. Biosci.* 165, 1–25.
- Hadeler, K.P., van den Driessche, P., 1997. Backward bifurcation in epidemic control. *Math. Biosci.* 146, 15–35.
- Hale, J.K., 1969. *Ordinary Differential Equations*. John Wiley&Sons, New York.
- Kribs-Zaleta, C.M., Martcheva, M., 2002. Vaccination strategies and backward bifurcation in an age-since-infection structured model. *Math. Biosci.* 177–178, 317–332.
- Kribs-Zaleta, C.M., Velasco-Hernandez, J., 2000. A simple vaccination model with multiple endemic states. *Math. Biosci.* 164, 183–201.
- Martcheva, M., Thieme, H.R., 2003. Progression age enhanced backward bifurcation in an epidemic model with super-infection. *J. Math. Biol.* 46, 385–424.
- Medley, G.F., Lindop, N.A., Edmunds, W.J., Nokes, D.J., 2001. Hepatitis-B virus endemicity: heterogeneity, catastrophic dynamics and control. *Nat. Med.* 7, 619–624.
- Mortreux, F., Gabet, A.-S., Wattel, E., 2003. Molecular and cellular aspects of HTLV-I associated leukemogenesis in vivo. *Leukemia* 17, 26–38.
- Mortreux, F., Kazanji, M., Gabet, A.-S., de Thoisy, B., Wattel, E., 2001. Two-step nature of human T-cell leukemia virus type 1 replication in experimentally infected squirrel monkeys (*Saimiri sciureus*). *J. Virol.* 75, 1083–1089.
- Nelson, P.W., Murray, J.D., Perelson, A.S., 2000. A model of HIV-1 pathogenesis that includes an intracellular delay. *Math. Biosci.* 163, 201–215.
- Nowak, M.A., May, R.M., 2000. *Virus Dynamics*. Oxford University Press, Oxford.
- Perelson, A.S., 1989. Modeling the interaction of the immune system with HIV. In: Castillo-Chavez, C. (Ed.), *Mathematical and Statistical Approaches to AIDS Epidemiology*. Lect. Notes Biomath, vol. 83. Springer, Berlin, pp. 350–370.
- Pugliese, A., 1990. Population models for diseases with no recovery. *J. Math. Biol.* 28, 65–82.
- van den Driessche, P., Watmough, J., 2000. A simple SIS epidemic model with a backward bifurcation. *J. Math. Biol.* 40, 525–540.
- Wang, L., Li, M.Y., Kirschner, D., 2002. Mathematical analysis of the global dynamics of a model for HTLV-I infection and ATL progression. *Math. Biosci.* 179, 207–217.
- Wattel, E., Vartanian, J.-P., Pannetier, C., Wain-Hobson, S., 1995. Clonal expansion of human T-cell leukemia virus type I-infected cells in asymptomatic and symptomatic carriers without malignancy. *J. Virol.* 69, 2863–2868.
- Wodarz, D., Nowak, M.A., Bangham, C.R.M., 1999. The dynamics of HTLV-I and the CTL response. *Immun. Today* 20, 220–227.
- Wucherpfennig, K.W., Höllsberg, P., Richardson, J.H., Benjamin, D., Hafler, D.A., 1992. T-cell activation by autologous human T-cell leukemia virus type I-infected T-cell clones. *Proc. Natl. Acad. Sci. USA* 89, 2110–2114.